CHAPTER 3

Photo-heating and supernova feedback amplify each other's effect on the cosmic star formation rate

Andreas H. Pawlik & Joop Schaye

P HOTO-HEATING associated with reionisation and kinetic feedback from core-collapse supernovae have previously been shown to suppress the high-redshift cosmic star formation rate. Here we investigate the interplay between photo-heating and supernova feedback using a set of cosmological, smoothed particle hydrodynamics simulations. We show that photo-heating and supernova feedback mutually amplify each other's ability to suppress the star formation rate. Our results demonstrate the importance of the simultaneous, non-independent inclusion of these two processes in models of galaxy formation to estimate the strength of the total negative feedback they exert. They may therefore be of particular relevance to semi-analytic models in which the effects of photo-heating and supernova feedback are implicitly assumed to act independently of each other.

3.1 INTRODUCTION

The cosmic star formation rate (SFR) is an important observable of our Universe. It is affected by a variety of physical processes, many of which are in turn regulated by the SFR, giving rise to so-called feedback loops (for an overview see, e.g., Ciardi & Ferrara 2005). Photo-ionisation heating due to the absorption of ionising photons from star-forming regions and the injection of kinetic energy from supernova (SN) explosions of massive stars provide two such feedback loops. Their implications for the assembly of the first generation of galaxies have been extensively discussed in studies of the epoch of reionisation (for a review of this epoch see, e.g., Loeb & Barkana 2001).

Photo-heating associated with reionisation increases the mean temperature of the intergalactic medium (IGM) to $\sim 10^4$ K (e.g., Hui & Gnedin 1997) and reduces the rate at which hotter gas can cool (Efstathiou 1992; Wiersma, Schaye, & Smith 2009). The increase in the gas temperature keeps the IGM smooth and prevents the assembly of low-mass galaxies, that is, galaxies with masses corresponding to a virial temperature $\lesssim 10^4$ K (e.g., Shapiro, Giroux, & Babul 1994; Gnedin & Hui 1998). Moreover, the gas in galaxies that have already collapsed is relatively quickly photo-evaporated (e.g., Shapiro, Iliev, & Raga 2004; Iliev, Shapiro, & Raga 2005), strongly decreasing the gas fraction of low-mass halos (e.g., Thoul & Weinberg 1996; Barkana & Loeb 1999; Dijkstra et al. 2004; Susa & Umemura 2006). Indeed, the cosmic SFR has been predicted to exhibit a distinct drop around the redshift of reionisation (Barkana & Loeb 2000). Photo-ionisation heating is therefore said to provide a negative feedback on reionisation.[1]

SN explosions of massive stars typically inject a few solar masses of gas with velocity of $\sim 10^4$ km s^{-1}, corresponding to a kinetic energy of $\sim 10^{51}$ erg. The ejected material sweeps up and shock-heats the surrounding gas, entraining outflows sufficiently powerful to, at least temporarily, substantially reduce the gas fractions for galaxy-scale dark matter halos (e.g., Yepes et al. 1997; Scannapieco et al. 2006). Since this leads to a suppression of the SFR, SN explosions, like photo-heating from reionisation, provide a negative feedback on reionisation. In addition to the depth of the gravitational potential, the ability of SN feedback to reduce the gas fractions generally depends on the geometry of the gas distribution (e.g., Mac Low & Ferrara 1999).

Studies of the effects of photo-heating and SN feedback on the SFR that considered each process in isolation have been augmented by studies that included both photo-heating and SN feedback. These studies include simulations of the formation of the first stars (e.g., Greif et al. 2007; Wise & Abel 2008; Whalen et al. 2008), of the evolution of isolated galaxies (e.g., Fujita et al. 2004; Dalla Vecchia & Schaye 2008, Tasker & Bryan 2008), and of galaxies in a cosmological volume (e.g., Tassis et al. 2003). Some of these studies also investigate the interplay between photo-heating and SN feedback. For example, Kitayama & Yoshida (2005) demonstrated in a one-dimensional hydrodynamical study that a previous episode of photo-heating may increase the efficiency of the evacuation of dark matter halos by (thermal) SN feedback and enable the destruction of galaxies out to much larger masses. In this chapter we report on another interaction of star formation feedbacks, using three-dimensional galaxy formation simulations.

We employ a set of Smoothed Particle Hydrodynamics (SPH) cosmological simulations that include star formation, and photo-ionisation heating from a uniform ultraviolet (UV) background and/or kinetic feedback from core-collapse SNe. We investigate how photo-heating af-

---

[1]As pointed out by Pawlik, Schaye, & van Scherpenzeel (2008), photo-heating also provides a strong positive feedback on reionisation because the increase in the gas temperature smoothes out density fluctuations, reducing the recombination rate.

Table 3.1: Simulation parameters. From left to right, table entries are: simulation label; comoving size of the simulation box, L_{box}; number of DM particles, N_{dm}; mass of dark matter particles, m_{dm}. A prefix *r9* indicates the inclusion of photo-heating in the optically thin limit from a uniform UV background (for $z \leq 9$) and a suffix *winds* indicates the inclusion of SN feedback (with initial wind velocity $v_{\text{w}} = 600$ km s^{-1} and mass loading $\eta = 2$). A bold font marks our set of reference simulations.

simulation	L_{box}	N_{dm}	m_{dm}
	[h^{-1} Mpc]		[$10^5 \ h^{-1} \ M_\odot$]
L6N256	**6.25**	**256^3**	**8.6**
r9L6N256	**6.25**	**256^3**	**8.6**
L6N256winds	**6.25**	**256^3**	**8.6**
r9L6N256winds	**6.25**	**256^3**	**8.6**
L3N256	3.125	256^3	1.1
r9L3N256	3.125	256^3	1.1
L3N256winds	3.125	256^3	1.1
r9L3N256winds	3.125	256^3	1.1
L3N128	3.125	128^3	8.6
r9L3N128	3.125	128^3	8.6
L3N128winds	3.125	128^3	8.6
r9L3N128winds	3.125	128^3	8.6

fects the high-redshift ($z \geq 6$) SFR in the presence and absence of SN feedback and, conversely, how SN feedback affects the cosmic SFR in the presence and absence of a photo-ionising background. We find that the inclusion of SN feedback amplifies the suppression of the cosmic SFR due to the inclusion of photo-heating. On the other hand, the inclusion of photo-heating amplifies the suppression of the cosmic SFR due to the inclusion of SN feedback.

Photo-heating and SN feedback therefore mutually amplify each other in suppressing the SFR. Our results are relevant to current implementations of (semi-) analytic models of galaxy formation (see Baugh 2006 for a review), in which the effects of photo-heating and SN feedback are implicitly assumed to act independently of each other. These models may thus underestimate the strength of the combined negative feedback from photo-heating and SNe.

We emphasise that none of our simulations has a sufficiently high resolution to achieve convergence in the cosmic SFR. Future simulations will therefore be required to quantify our qualitative statement. We show, however, that the factor by which photo-heating and SN feedback amplify each other's ability to suppress the cosmic SFR becomes larger with increasing resolution, giving credibility to our main conclusion.

This chapter is organised as follows. We present our simulation method in §3.2 and we illustrate our main result in §3.3. Finally, we summarize our conclusions and discuss the caveats inherent to the present work in §3.4.

3.2 Simulations

Our simulation method is identical to that employed in Pawlik, Schaye, & van Scherpenzeel (2008), to which we refer the reader for more details. We use a modified version of the N-body/TreePM/SPH code GADGET-2 (Springel 2005) to perform a total of 12 cosmological SPH simulations at different resolutions, using different box sizes. We employ the set of cosmologi-

cal parameters $[\Omega_m, \Omega_b, \Omega_\Lambda, \sigma_8, n_s, h]$ given by $[0.258, 0.0441, 0.742, 0.796, 0.963, 0.719]$, in agreement with the WMAP 5-year observations (Komatsu et al. 2008). The simulations include radiative cooling, star formation and, optionally, photo-heating by a uniform UV background and/or kinetic feedback from SNe (see Table 3.1).

The gas is of primordial composition and is allowed to cool by collisional ionisation and excitation, emission of free-free and recombination radiation and Compton cooling off the cosmic microwave background. Molecular hydrogen is kept photo-dissociated at all times by the inclusion of a soft UV background. We employ the star formation recipe of Schaye & Dalla Vecchia (2008), to which we refer the reader for details. According to this recipe, gas forms stars at a pressure-dependent rate that reproduces the observed Kennicutt-Schmidt law (Kennicutt 1998).

Photo-ionisation (heating) is included in the optically thin limit using a uniform Haardt & Madau (2001) UV background from quasars and galaxies for redshifts $z \leq z_r = 9$. The value for z_r is consistent with the most recent determination of the Thomson optical depth towards reionisation from the WMAP (5-year) experiment (Komatsu et al. 2008). We inject an additional thermal energy of 2 eV per proton at $z = z_r$. In the absence of shocks, gas particles at the cosmic mean density are therefore kept at a temperature $T \approx 10^4$ K for $z < z_r$ (see Fig. 1 of Pawlik, Schaye, & van Scherpenzeel 2008).

We model kinetic feedback from star formation using the prescription of Dalla Vecchia & Schaye (2008), according to which core-collapse SNe locally inject kinetic energy and kick gas particles into winds. The feedback is specified by two parameters, the initial wind mass loading in units of the newly formed stellar mass, η, and the initial wind velocity v_w. We adopt $\eta = 2$ and $v_w = 600$ km s^{-1}, consistent with observations of local (e.g. Veilleux, Cecil, & Bland-Hawthorn 2005) and redshift $z \approx 3$ (e.g. Shapley et al. 2003) starburst galaxies. This choice of parameters implies that 40 per cent of the energy available from core-collapse SNe is injected as kinetic energy (assuming a Chabrier initial mass function in the range $0.1 \leq M/M_\odot \leq 100$ and 10^{51} erg per $M > 6 \, M_\odot$ star), while the remaining 60 per cent are implicitly assumed to be lost radiatively.

We use a Friends-of-Friends halo finder (Davis et al. 1985) with linking length $b = 0.2$ to obtain a list of dark matter halos contained in each of our simulation outputs. Only halos containing more than 100 dark matter particles are included in these lists. For each simulation output we compute the SFR associated with dark matter halo as follows. First, gas particles are attached to the nearest dark matter particle. Second, the SFR of a dark matter halo is the sum of the SFRs of the gas particles that were attached to the dark matter particles it contains.

3.3 RESULTS

Our main result is shown in Fig. 3.1. The top panel shows the evolution of the total SFR, defined as the sum of the star formation rates over all halos, for our set of reference simulations. We use $\dot{\rho}_{*,wh}$, $\dot{\rho}_{*,h}$ and $\dot{\rho}_{*,w}$ to denote, respectively, the SFR densities in the simulations with both SN feedback and photo-heating (red dashed curve, *r9L6N256winds*), with photo-heating but without SN feedback (red solid curve, *r9L6N256*) and with SN feedback but without photo-heating (blue dashed curve, *L6N256winds*). We denote the SFR density in the simulation that included neither photo-heating nor wind feedback with $\dot{\rho}_*$ (blue solid curve, *L6N256*).

Both the inclusion of photo-heating and the inclusion of kinetic feedback from SNe lead to a significant suppression of the SFR. The factor $s_h \equiv \dot{\rho}_*/\dot{\rho}_{*,h}$ by which the SFR is suppressed due to photo-heating is smaller than the factor $s_w \equiv \dot{\rho}_*/\dot{\rho}_{*,w}$ by which the SFR is suppressed due to
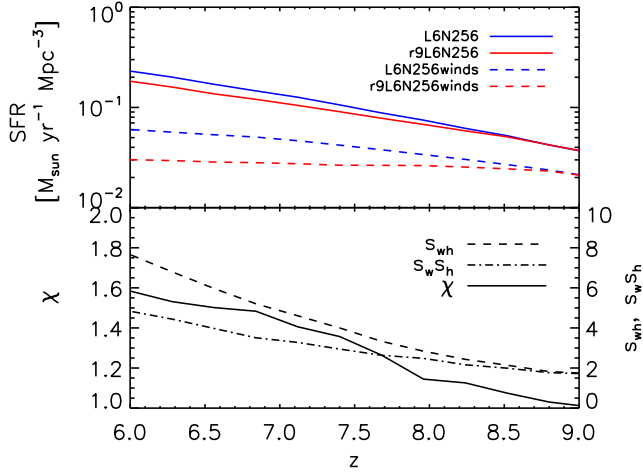
Figure 3.1: Top panel: evolution of the total SFRs in our set of reference simulations. Photo-heating and SN feedback were included for the red and dashed curves, respectively. Star formation is strongly suppressed when photo-heating and/or kinetic feedback from SNe are included. Bottom panel: Suppression factors s_{wh} and $s_{\mathrm{w}}s_{\mathrm{h}}$ (right y-axis) and feedback amplification factor $\chi \equiv s_{\mathrm{wh}}/(s_{\mathrm{w}}s_{\mathrm{h}})$ (left y-axis). The fact that $\chi > 1$ implies that photo-heating and SN feedback amplify each other's ability to suppress the SFR.

kinetic feedback. As expected, the simultaneous inclusion of photo-heating and feedback from SNe leads to a suppression of the SFR by a factor $s_{\mathrm{wh}} \equiv \dot{\rho}_*/\dot{\rho}_{*,\mathrm{wh}}$ that is larger than the factors s_{h} and s_{w} by which the SFRs are suppressed due to the sole inclusion of either photo-heating or SN feedback.

Interestingly, the factor by which the SFR is suppressed due to photo-heating is larger in the presence (set of dashed curves) than in the absence (set of solid curves) of SN feedback. Conversely, the factor by which the SFR is suppressed due to SN feedback is larger in the presence (set of red curves) than in the absence (set of blue curves) of photo-heating.

Photo-heating and SN feedback thus mutually amplify each other in suppressing the SFR. This amplification probably arises because the inclusion of photo-heating keeps the gas diffuse, which makes it easier for the winds to drag it out of halos. Winds, on the other hand, move gas from the central to the outer parts of halos, where it is more susceptible to the photo-evaporation process. Models that implicitly ignore this interaction between photo-heating and SN feedback, like for example (semi-) analytic models of galaxy formation (e.g., Khochfar & Ostriker 2008; Monaco, Fontanot, & Taffoni 2007; Benson et al. 2006; Croton et al. 2006; Benson et al. 2002; Somerville 2002), thus may underestimate the strength of the feedback these processes exert.

We now define the feedback amplification factor $\chi \equiv s_{\mathrm{wh}}/(s_{\mathrm{w}}s_{\mathrm{h}})$. A value $\chi = 1$ would indicate that photo-heating and SN feedback suppress the SFR independently of each other. A value $\chi > 1$ ($\chi < 1$) would indicate that photo-heating and SN feedback amplify (weaken) each other's ability to suppress the SFR. The evolution of the amplification factor χ is shown in the bottom panel of Fig. 3.1, together with that of s_{wh} and $s_{\mathrm{w}}s_{\mathrm{h}}$. The fact that $\chi > 1$ for $z < 9$ implies that photo-heating and SN feedback amplify each other in suppressing star formation.[2]

To demonstrate that this amplification is indeed mutual, we write $s_{\mathrm{wh}} \equiv s_{\mathrm{w|h}}s_{\mathrm{h}} \equiv s_{\mathrm{h|w}}s_{\mathrm{w}}$. This defines the suppression factors $s_{\mathrm{w|h}} = \dot{\rho}_{*,\mathrm{h}}/\dot{\rho}_{*,\mathrm{wh}}$ and $s_{\mathrm{h|w}} = \dot{\rho}_{*,\mathrm{w}}/\dot{\rho}_{*,\mathrm{wh}}$. Thus, $s_{\mathrm{w|h}}$ is the factor by which SN feedback suppresses the SFR in simulations that include photo-heating and $s_{\mathrm{h|w}}$ is the factor by which photo-heating suppresses the SFR in simulations that include SN feedback. We have

$$\frac{s_{\mathrm{w|h}}}{s_{\mathrm{w}}} = \frac{\dot{\rho}_{*,\mathrm{h}}/\dot{\rho}_{*,\mathrm{wh}}}{\dot{\rho}_*/\dot{\rho}_{*,\mathrm{w}}} = \frac{\dot{\rho}_{*,\mathrm{w}}/\dot{\rho}_{*,\mathrm{wh}}}{\dot{\rho}_*/\dot{\rho}_{*,\mathrm{h}}} = \frac{s_{\mathrm{h|w}}}{s_{\mathrm{h}}}. \tag{3.1}$$

---

[2]Note that in our simulations $s_{\mathrm{h}} = 1 = \chi$ for $z \geq 9$ because there is no photo-heating at these redshifts.

This shows explicitly that the amplification of the suppression of the SFR due to photo-heating in simulations that include SN feedback is equal to the amplification of the suppression of the SFR due to SN feedback in simulations that include photo-heating. It implies that we cannot determine whether photo-heating amplifies the effect of SN feedback or vice versa.

Fig. 3.2 shows, for our set of reference simulations, the dependence of the suppression of the SFR due to photo-heating and/or SN feedback on halo mass. The top panel shows the cumulative SFR at $z = 6$ in dark matter halos less massive than M_{dm}. The bottom panel shows, similar to the bottom panel of Fig. 3.1, the feedback amplification factor χ obtained from analogous definitions of the suppression factors $s_{\mathrm{h}}, s_{\mathrm{w}}$ and s_{wh} applied to the cumulative SFR at $z = 6$ shown in the top panel. The vertical dotted lines indicate the dark matter mass corresponding to a virial temperature $T_{\mathrm{vir}} = 10^4$ K.

While photo-heating strongly decreases the SFR in halos with virial temperatures $T_{\mathrm{vir}} \lesssim 10^4$ K, the inclusion of SN feedback leads to a strong decrease in the SFR in halos with $T_{\mathrm{vir}} \gtrsim 10^4$ K. Radiative and kinetic feedback thus act mostly over complementary mass ranges. This dichotomy arises because photo-evaporation mainly affects the gas fractions of halos with masses that correspond to virial temperatures that are of order of or smaller than the thermal temperature to which the gas is photo-heated, $T_{\mathrm{vir}} \lesssim 10^4$ K. In contrast, star formation and the associated SN feedback become only efficient for halos with masses corresponding to $T_{\mathrm{vir}} \gtrsim 10^4$ K, because our simulations do not include radiative cooling from metals and molecules (and because of our limited resolution), which could potentially enable star formation in halos of much smaller virial temperatures.

The left-hand (right-hand) panels of Fig. 3.3 show the evolution (mass-dependence) of the feedback amplification factor χ obtained from simulations for which we have varied the size of the simulation box and/or the resolution. Note that the solid, black curves in the left-hand and right-hand panels are identical to the solid, black curves shown in the bottom panels of Figs. 3.1 and 3.2, respectively.

Changing the size of the simulation box by a factor of two (at fixed resolution; solid curves) has little effect. On the other hand, increasing the resolution by a factor of two (while keeping the size of the simulation box fixed; red curves) significantly increases χ. The increase in χ with increasing resolution is likely due to both an increase in the fraction of galaxies that are subject to photo-evaporation and an increase in the SFR (and thus associated SN feedback) of all galaxies.

3.4 DISCUSSION

Photo-heating from reionisation and supernova (SN) feedback are key processes that determine the star formation rate (SFR) in the high-redshift Universe. Using a set of cosmological SPH simulations that include radiative cooling and star formation, we analysed the $z \geq 6$ star formation history in the presence of photo-ionisation heating from a uniform UV background and/or kinetic feedback from core-collapse SNe. The inclusion of photo-heating and SN feedback both lead to a suppression of the SFR.

We showed that the factor by which the SFR is suppressed due to photo-heating is larger in the presence than in the absence of SN feedback. We also showed that the factor by which the SFR is suppressed due to the inclusion of SN feedback is larger in the presence than in the absence of photo-heating. This mutual amplification of SN feedback and reionisation heating is the central result of the present work.

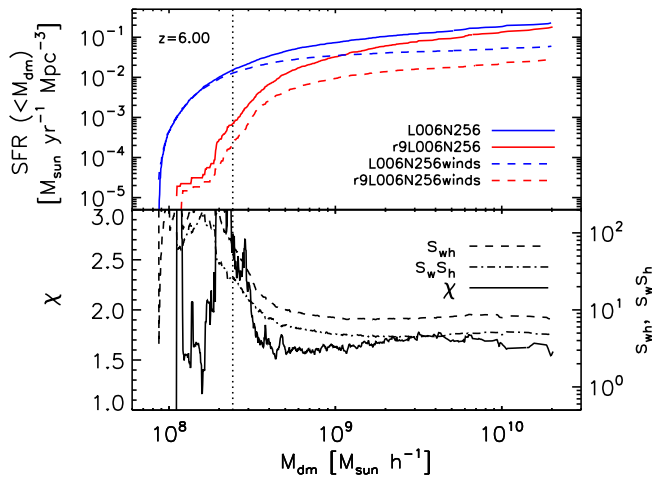We caution the reader that our simulations have not fully converged with respect to res-

Figure 3.2: Top panel: cumulative SFRs as function of dark matter halo mass at $z = 6$ for our set of reference simulations. Photo-heating and SN feedback suppress the SFR over roughly complementary mass ranges. Bottom panel: similar to the bottom panel of Fig. 3.1, but now for the cumulative SFRs shown in the top panel. The vertical dotted lines indicate the dark matter mass corresponding to a virial temperature $T_{\rm vir} = 10^4$ K.
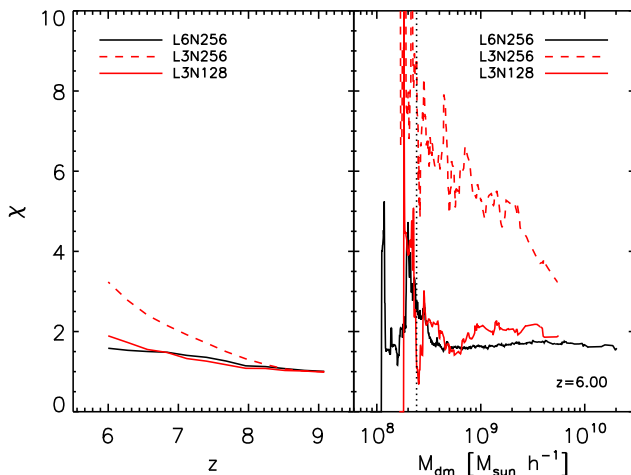

Figure 3.3: Evolution (left-hand panel) and mass-dependence (at $z = 6$; right-hand panel) of the feedback amplification factor χ for different choices of the box size and resolution. The vertical, dotted line in the right panel indicates the dark matter mass corresponding to a virial temperature $T_{\rm vir} = 10^4$ K. The feedback amplification factor is insensitive to the size of the simulation box but increases strongly with resolution.

olution and that we have ignored some potentially important physical processes. This result will therefore need to be confirmed and quantified with future simulations. In what follows we briefly discuss the most important physical effects that our analysis ignored.

We computed photo-heating rates from a uniform UV background in the optically thin limit. Our simulations therefore do not account for the self-shielding of gas from ionising radiation. This may lower the fraction of the gas that is photo-evaporated (e.g., Kitayama et al. 2000; Susa & Umemura 2004; Dijkstra et al. 2004). Iliev, Shapiro, & Raga (2005) (extending the work of Shapiro, Iliev, & Raga 2004) have, however, pointed out that regions that are initially self-shielded will eventually also be photo-evaporated: as subsequent layers of gas are photo-evaporated, previously self-shielded regions become exposed to ionising radiation and are eventually stripped away. Moreover, the evaporation of the initially self-shielded gas may proceed at a speed comparable to the speed predicted by simulations that compute photo-heating rates in the optically thin limit (Fig. 3 in Iliev, Shapiro, & Raga 2005). Note also that because SN explosions decrease the gas density, the effects of self-shielding may be less prominent in simulations that include this type of feedback. Clearly, the importance of self-shielding and the applicability of the optically thin limit to the present problem need to be critically as-

sessed using cosmological radiation-hydrodynamical simulations.

Although all of our simulations employ a sufficiently high resolution to resolve all halos with virial temperatures $T_{\rm vir} \gtrsim 10^4$ K with at least 100 particles, none of them has the resolution to properly reproduce the properties of the multi-phase medium associated with the star-forming regions these halos host. The factors by which photo-heating and SN feedback suppress the SFR are therefore not yet converged. We have, however, demonstrated that the effect of mutual amplification of photo-heating and SN feedback becomes only stronger with increasing resolution.

Because we have assumed the presence of a photo-dissociating background, the formation of molecular hydrogen is suppressed in our simulations. In reality, the gas may contain a significant fraction of molecular hydrogen before reionisation (but see, e.g., Haiman, Rees, & Loeb 1997). Star formation and the associated kinetic feedback would then already be efficient in halos with virial temperatures much smaller than 10^4 K (e.g., Tegmark et al. 1997). Because the gas fraction in these halos would be affected by both photo-heating and SN feedback, we expect that the inclusion of molecular hydrogen would only strengthen our main result.

We have also ignored the existence of atoms and ions heavier than helium. SN explosions may, however, quickly enrich the interstellar and intergalactic gas with metals (e.g., Bromm, Yoshida, & Hernquist 2003), which would increase its ability to cool. Metal enrichment thus provides a positive feedback that may partially offset the negative kinetic feedback from SN explosions.

None of the caveats we discussed seems, however, likely to invalidate our main qualitative conclusion that photo-heating and SN explosions amplify each other's effect on the cosmic SFR. Galaxy formation models that treat the effects of photo-heating and SN explosions independently of each other, like e.g. (semi-) analytic models, may therefore significantly underestimate the effect of these feedback processes on the SFR. Because photo-heating and SN feedback are important processes that affect the gas in low mass-halos at all epochs, our findings may also have implications for the understanding of the properties of low-redshift galaxies, e.g. in the context of the missing satellite problem (for a recent discussion see, e.g., Koposov et al. 2009).

REFERENCES

Barkana R., Loeb A., 1999, ApJ, 523, 54

Barkana R., Loeb A., 2000, ApJ, 539, 20

Baugh C. M., 2006, RPPh, 69, 3101

Benson A. J., Sugiyama N., Nusser A., Lacey C. G., 2006, MNRAS, 369, 1055

Benson A. J., Lacey C. G., Baugh C. M., Cole S., Frenk C. S., 2002, MNRAS, 333, 156

Bromm V., Yoshida N., Hernquist L., 2003, ApJ, 596, L135

Ciardi B., Ferrara A., 2005, SSRv, 116, 625

Croton D. J., et al., 2006, MNRAS, 365, 11

Dalla Vecchia C., Schaye J., 2008, MNRAS, 387, 1431

Davis M., Efstathiou G., Frenk C. S., White S. D. M., 1985, ApJ, 292, 371

Dijkstra M., Haiman Z., Rees M. J., Weinberg D. H., 2004, ApJ, 601, 666

Efstathiou G., 1992, MNRAS, 256, 43P

Fujita A., Mac Low M.-M., Ferrara A., Meiksin A., 2004, ApJ, 613, 159

Gnedin N. Y., Hui L., 1998, MNRAS, 296, 44

Greif T. H., Johnson J. L., Bromm V., Klessen R. S., 2007, ApJ, 670, 1

Haardt F., Madau P., 2001, in Neumann D. M.,Van J. T. T., eds, Proc.XXXVI Rencontres de Moriond, Clusters of Galaxies and the High Redshift Universe Observed in X-Rays, preprint (astro-ph/0106018)

Haiman Z., Rees M. J., Loeb A., 1997, ApJ, 476, 458

Hui L., Gnedin N. Y., 1997, MNRAS, 292, 27

Iliev I. T., Shapiro P. R., Raga A. C., 2005, MNRAS, 361, 405

Kennicutt R. C., Jr., 1998, ApJ, 498, 541

Kitayama T., Tajiri Y., Umemura M., Susa H., Ikeuchi S., 2000, MNRAS, 315, L1

Kitayama T., Yoshida N., 2005, ApJ, 630, 675

Khochfar S., Ostriker J. P., 2008, ApJ, 680, 54

Komatsu E., et al., 2008, preprint (arXiv:0803.0547)

Koposov S. E., Yoo J., Rix H.-W., Weinberg D. H., Macciò A. V., Miralda-Escudé J., 2009, preprint (arXiv:0901.2116)

Loeb A., Barkana R., 2001, ARA&A, 39, 19

Mac Low M.-M., Ferrara A., 1999, ApJ, 513, 142

Monaco P., Fontanot F., Taffoni G., 2007, MNRAS, 375, 1189

Pawlik A. H, Schaye J., van Scherpenzeel, E., MNRAS, in press, preprint (arXiv:0807.3963)

Scannapieco C., Tissera P. B., White S. D. M., Springel V., 2006, MNRAS, 371, 1125

Schaye J., Dalla Vecchia C., 2008, MNRAS, 383, 1210

Shapiro P. R., Giroux M. L., Babul A., 1994, ApJ, 427, 25

Shapiro P. R., Iliev I. T., Raga A. C., 2004, MNRAS, 348, 753

Shapley A. E., Steidel C. C., Pettini M., Adelberger K. L., 2003, ApJ, 588, 65

Somerville R. S., 2002, ApJ, 572, L23

Springel V., 2005, MNRAS, 364, 1105

Susa H., Umemura M., 2004, ApJ, 600, 1

Susa H., Umemura M., 2006, ApJ, 645, L93

Tasker E. J., Bryan G. L., 2008, ApJ, 673, 810

Tassis K., Abel T., Bryan G. L., Norman M. L., 2003, ApJ, 587, 13

Tegmark M., Silk J., Rees M. J., Blanchard A., Abel T., Palla F., 1997, ApJ, 474, 1

Thoul A. A., Weinberg D. H., 1996, ApJ, 465, 608

Veilleux S., Cecil G., Bland-Hawthorn J., 2005, ARA&A, 43, 769

Wiersma R. P. C., Schaye J., Smith B. D., 2009, MNRAS, 393, 99

Whalen D., van Veelen B., O'Shea B. W., Norman M. L., 2008, ApJ, 682, 49

Wise J. H., Abel T., 2008, ApJ, 685, 40

Yepes G., Kates R., Khokhlov A., Klypin A., 1997, MNRAS, 284, 235